



Dielectric properties of B_2O_3 -doped $0.92(Mg_{0.95}Co_{0.05})_2TiO_4-0.08(Ca_{0.8}Sr_{0.2})TiO_3$ ceramics for microwave applications

Bing-Jing Li, Jhih-Yong Chen, Guan-Sian Huang, Chang-Yang Jiang, Cheng-Liang Huang*

Department of Electrical Engineering, National Cheng Kung University, No. 1 University Road, Tainan 70101, Taiwan

ARTICLE INFO

Article history:

Received 24 February 2010
Received in revised form 6 June 2010
Accepted 9 June 2010
Available online 18 June 2010

Keywords:

Crystal growth
Dielectric response

ABSTRACT

The dielectric properties and microstructures of $0.92(Mg_{0.95}Co_{0.05})_2TiO_4-0.08(Ca_{0.8}Sr_{0.2})TiO_3$ ceramics with B_2O_3 additions have been investigated. The sintered $0.92(Mg_{0.95}Co_{0.05})_2TiO_4-0.08(Ca_{0.8}Sr_{0.2})TiO_3$ ceramics were characterized by using X-ray diffraction spectra, scanning electron microscopy (SEM), backscattering electron image (BEI) and energy dispersive X-ray (EDX). The dielectric properties are strongly dependent on the densifications and the microstructures of the specimens. The decrease of $Q \times f$ value at high-level B_2O_3 addition was owing to the inhomogeneous grain growth and the high-dielectric-loss of the liquid phase. In comparison with that of pure $0.92(Mg_{0.95}Co_{0.05})_2TiO_4-0.08(Ca_{0.8}Sr_{0.2})TiO_3$ ceramics, specimen with 0.5 wt% B_2O_3 addition possesses a substantial fine combination of dielectric properties (an ϵ_r of 18.07, a $Q \times f$ of 95,000 GHz at 9.5 GHz and a τ_f of -4.7 ppm/ $^{\circ}C$) at a lower sintering temperature of $1200^{\circ}C$ for 4 h. Moreover, a band-pass filter is also designed and simulated on the proposed dielectric to study its performance.

© 2010 Elsevier B.V. All rights reserved.

1. Introduction

Low-loss microwave dielectrics with dielectric constant in the 20 s have become one of the most popular materials used for today's GPS patch antennas and 3G filters [1–3]. These dielectric resonators, however, must satisfy three main criteria: a high-dielectric constant (ϵ_r) for miniaturization, a high quality factor ($Q \times f$) for better selectivity, and a near-zero temperature coefficient of resonant frequency (τ_f) for stable frequency stability [4,5]. In particular, high quality factor (inverse of the dielectric loss, $Q = 1/\tan \delta$) would play a more prominent role for high frequency applications [6,7]. Research of new materials that satisfy such a requirement has been ongoing and has been reported in the last few years. For instance, $MgTiO_3$ and Mg_2TiO_4 , belonging to the $MgO-TiO_2$ binary system, are both recognized as good candidates for high frequency applications [8–11].

Mg_2TiO_4 -based ceramics have wide applications as dielectrics in resonators, filters and antennas for communication, radar and global positioning systems operating at microwave frequencies.

Mg_2TiO_4 has a spinel-type structure and a space group of $Fd-3m$ (227) [11,12]. Partially replacing Mg by Co, the $(Mg_{0.95}Co_{0.05})_2TiO_4$ ceramic possesses a high-dielectric constant (ϵ_r) of ~ 15.7 , a high $Q \times f$ value of $\sim 286,000$ GHz (at 10.4 GHz) and a negative τ_f value of -52.5 ppm/ $^{\circ}C$ [13]. Dielectrics such as $CaTiO_3$, $SrTiO_3$ and $(Ca_{0.8}Sr_{0.2})TiO_3$ ($\epsilon_r \sim 181$, $Q \times f$ value ~ 8300 GHz and τ_f value ~ 991 ppm/ $^{\circ}C$) [14] have been individually employed as an effective τ_f compensator for materials having positive τ_f , such as $MgTiO_3$, Mg_2TiO_4 , $La(Zn_{1/2}Ti_{1/2})O_3$ and $Ca(Mg_{1/3}Nb_{2/3})O_3$ [8,15–17]. In our previous report, $0.92(Mg_{0.95}Co_{0.05})_2TiO_4-0.08(Ca_{0.8}Sr_{0.2})TiO_3$ ceramic could possess a good combination of dielectric properties ($\epsilon_r \sim 19.22$, $Q \times f$ value $\sim 123,200$ GHz (at 9.2 GHz) and $\tau_f \sim 2.8$ ppm/ $^{\circ}C$) [18]. However, it required a high sintering temperature of $1300^{\circ}C$. The chemical processing and the use of small particles of starting materials normally can reduce the sintering temperature of dielectric materials. However, these required a flexible procedure that would increase the cost and time for the fabrication of dielectric resonators. Liquid phase sintering by adding glass or other materials with a low melting point also can effectively lower the firing temperature of the ceramics [19,20].

In the present study, B_2O_3 was selected as a sintering aid to lower the sintering temperature of $0.92(Mg_{0.95}Co_{0.05})_2TiO_4-0.08(Ca_{0.8}Sr_{0.2})TiO_3$ ceramics. The dielectric properties at

* Corresponding author. Tel.: +886 6 2757575x62390; fax: +886 6 2345482.
E-mail address: huangcl@mail.ncku.edu.tw (C.-L. Huang).

microwave frequencies of the sintered ceramics were characterized and discussed in terms of the densification and the B_2O_3 content of the specimens. In addition, the X-ray diffraction (XRD) patterns and the scanning electron microscopy (SEM) analysis were also employed to study the crystal structures and microstructures of the ceramics. The correlation between the microstructure and the $Q \times f$ value was also investigated.

2. Experimental procedure

Samples of $0.92(Mg_{0.95}Co_{0.05})_2TiO_4-0.08(Ca_{0.8}Sr_{0.2})TiO_3$ were synthesized by conventional solid-state methods from individual high-purity oxide powders (>99.9%): MgO , CoO , $CaCO_3$, $SrCO_3$ and TiO_2 . The starting materials were separately prepared according to the desired stoichiometry $(Mg_{0.95}Co_{0.05})_2TiO_4$ and $(Ca_{0.8}Sr_{0.2})TiO_3$, and ground in distilled water for 24 h in a ball mill with agate balls. All mixtures were dried and calcined at $1100^\circ C$ for 4 h. The calcined powders were then doped 0.5–2 wt% B_2O_3 ceramics and remilled for 24 h. The fine powder together with the organic binder was pressed into pellets with dimensions of 11 mm in diameter and 5 mm thickness under the pressure of $2000 kg/cm^2$. These pellets were sintered at temperature of $1110-1260^\circ C$ for 4 h in air.

The crystalline phases of the sintered ceramics were identified by XRD using $Cu K\alpha$ ($\lambda=0.15406 nm$) radiation with a Siemens D5000 diffractometer operated at 40 kV and 40 mA. The microstructure observations of sintered surface were performed by means of scanning electron microscopy (SEM), backscattering electron image (BEI) and an energy dispersive X-ray spectrometer (EDS). The apparent densities of the sintered pellets were measured by the Archimedes method. The dielectric constant (ϵ_r) and the quality factor values (Q) at microwave frequencies were measured using the Hakki-Coleman dielectric resonator method as modified and improved by Courtney [21,22]. A system combining a HP8757D network analyzer and a HP8350B sweep oscillator was employed in the measurement. An identical technique was applied to the measurement of the temperature coefficient of resonant frequency (τ_f). The test set was placed over a thermostat in the temperature range of $+25$ to $+80^\circ C$. τ_f (ppm/ $^\circ C$) can be calculated by considering the change in resonant frequency (Δf).

$$\tau_f = \frac{f_2 - f_1}{f_1(T_2 - T_1)} \quad (1)$$

where f_1 and f_2 represent the resonant frequencies at T_1 and T_2 , respectively.

3. Results and discussion

Fig. 1 shows the X-ray diffraction patterns of B_2O_3 -doped $0.92(Mg_{0.95}Co_{0.05})_2TiO_4-0.08(Ca_{0.8}Sr_{0.2})TiO_3$ (hereafter referred to as 92MCT–8CST) ceramics produced at different sintering temperatures. The $(Mg_{0.95}Co_{0.05})_2TiO_4$ was detected as the main crystalline phase associated with a minor phase $(Ca_{0.8}Sr_{0.2})TiO_3$ indicating the formation of a two-phase system. Moreover, the X-ray diffraction patterns of the 92MCT–8CST ceramics with 0.5 wt% B_2O_3 addi-

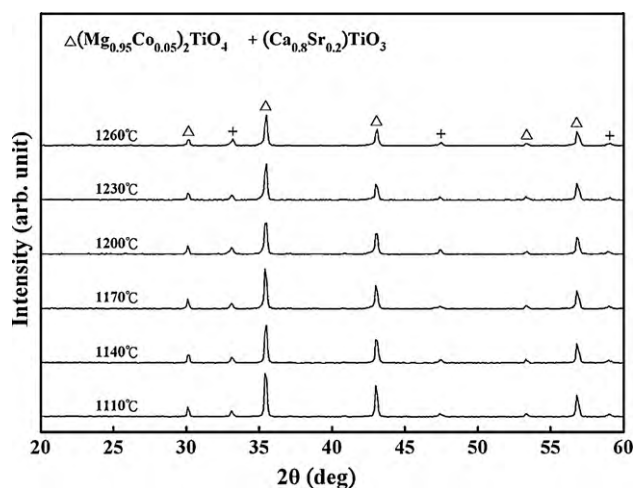


Fig. 1. X-ray diffraction patterns of $0.92(Mg_{0.95}Co_{0.05})_2TiO_4-0.08(Ca_{0.8}Sr_{0.2})TiO_3$ ceramics with 0.5 wt% B_2O_3 additions sintered at different temperatures for 4 h.

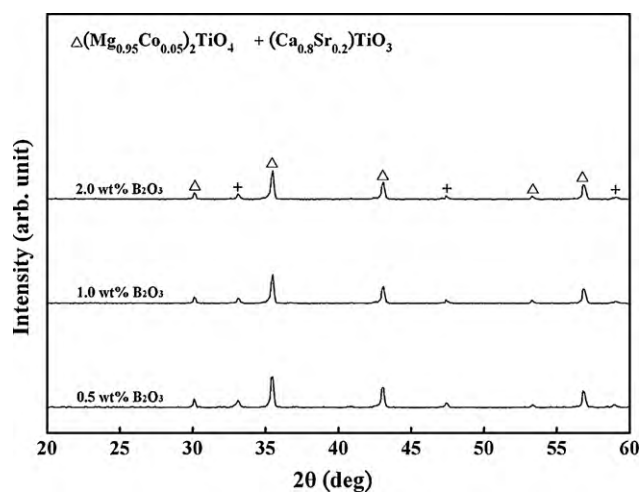


Fig. 2. X-ray diffraction patterns of $0.92(Mg_{0.95}Co_{0.05})_2TiO_4-0.08(Ca_{0.8}Sr_{0.2})TiO_3$ ceramics with different amount of B_2O_3 additions sintered at $1200^\circ C$ for 4 h.

tion have not change significantly with sintering temperature in the range from 1110 to $1260^\circ C$. The X-ray diffraction patterns of 92MCT–8CST ceramics with different amounts of B_2O_3 additions sintered at $1200^\circ C$ are illustrated in Fig. 2. Identical XRD patterns were observed for the ceramics irrespective of the amounts of B_2O_3 additions.

SEM micrographs of 0.5 wt% B_2O_3 -doped 92MCT–8CST with sintering temperature of $1110-1260^\circ C$ are presented in Fig. 3. The grain growth of 92MCT–8CST crystallites was enhanced with increasing sintering temperature. Compared to the microstructure of pure 92MCT–8CST at $1200^\circ C$ [18], the B_2O_3 -doped one also has a similar grain size but shows a well-developed microstructure. It is owing to the fact that the sintering aid promoted the densification of ceramic but inhibited the grain growth due to a higher surface energy. In addition, Fig. 4 illustrated the SEM micrographs of the 92MCT–8CST ceramics with different amounts of B_2O_3 additions at $1200^\circ C$. The grain size increased with the increase of sintering temperature as well as the amount of B_2O_3 addition due to the formation of liquid phase. These may directly affect the microwave dielectric properties of the 92MCT–8CST samples.

Energy dispersive X-ray (EDX) analysis was used in combination with backscattering electron image (BEI, Fig. 5) to distinguish each grain of 0.5 wt% B_2O_3 -doped 92MCT–8CST ceramics sintered at $1200^\circ C$. From the EDX analysis, the EDX datum of spots A–F was shown in Table 1. The grain morphology of 0.5 wt% B_2O_3 -doped 92MCT–8CST ceramics exhibited two types of grains: large grains (spots A–C) were $(Mg_{0.95}Co_{0.05})_2TiO_4$ and small cubic-shape grains (spots D–F) were $(Ca_{0.8}Sr_{0.2})TiO_3$. As can be seen, all the grains contain a small amount of B indicating the liquid phase will residual inside the grains at the final stage of sintering.

The apparent densities and ϵ_r of the B_2O_3 -doped 92MCT–8CST ceramics at different sintering temperatures are shown in Fig. 6. The apparent density increased with increasing sintering temperature, reaching the maximum at $1150-1200^\circ C$ and slightly decreased thereafter. The decrease of density was due to the appearance of pores resulted from an inhomogeneous grain morphology as shown in Fig. 3. The maximum density of $3.45 g/cm^3$ was achieved for specimen using 0.5 wt% B_2O_3 addition at $1200^\circ C$. The results suggest that a higher amount of B_2O_3 is not required for producing dense ceramics. Moreover, the variation of dielectric constant was consistent with that of density and a maximum ϵ_r of 18.07 was obtained for specimen using

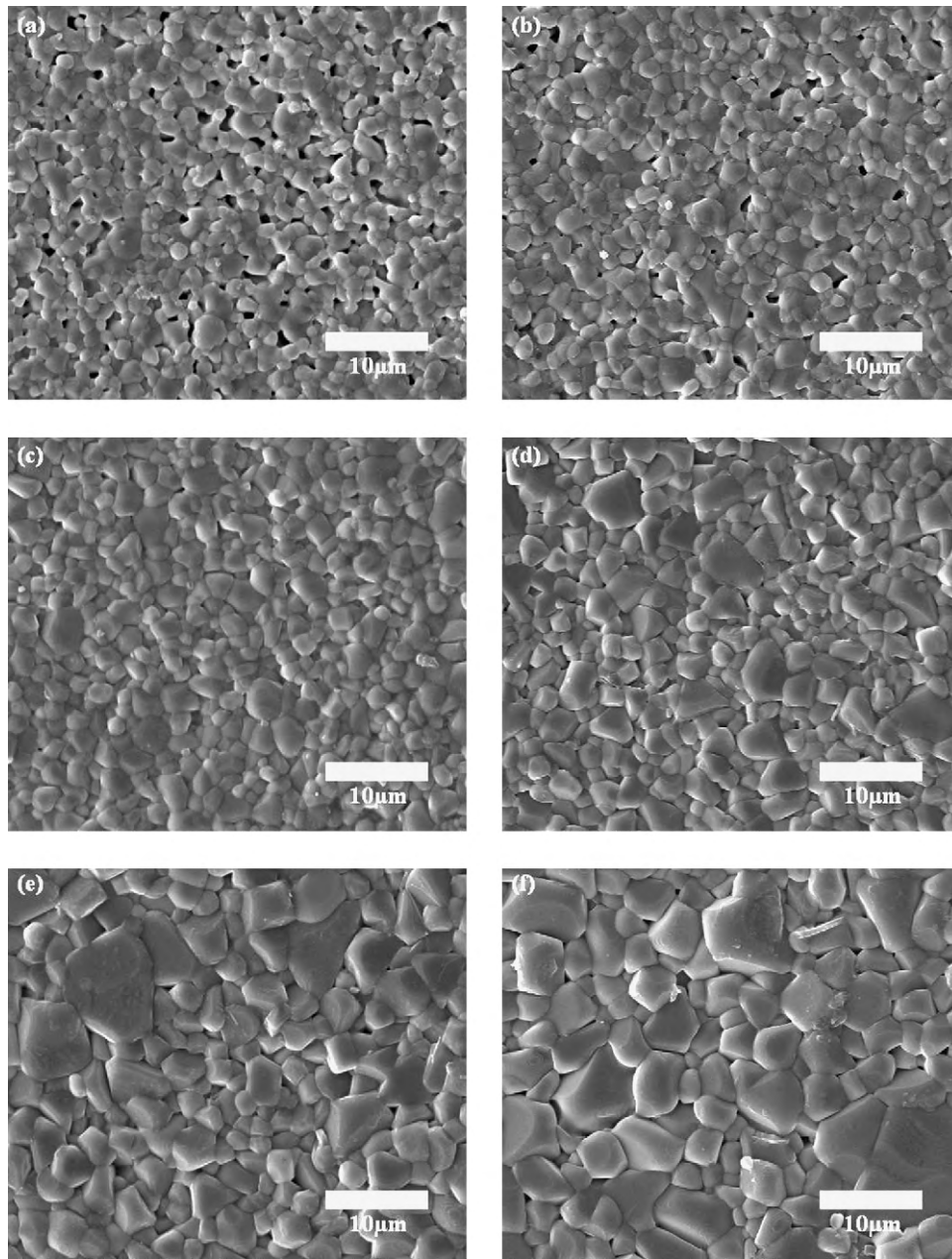


Fig. 3. SEM micrographs of $0.92(\text{Mg}_{0.95}\text{Co}_{0.05})_2\text{TiO}_4-0.08(\text{Ca}_{0.8}\text{Sr}_{0.2})\text{TiO}_3$ ceramics with 0.5 wt% B_2O_3 addition sintered at (a) 1110 °C, (b) 1140 °C, (c) 1170 °C, (d) 1200 °C, (e) 1230 °C and (f) 1260 °C for 4 h.

0.5 wt% B_2O_3 -doped 92MCT–8CST ceramics sintered at 1200 °C for 4 h. Being a sintering aid, B_2O_3 would enhance the densification resulted in an increase in the dielectric constant of the ceramics. However, too high a B_2O_3 doping level degraded its dielectric constant, which might be due to the low ϵ_r value of sintering aid.

Fig. 7 shows the quality factor ($Q \times f$) and τ_f of the B_2O_3 -doped 92MCT–8CST at different sintering temperatures. With increasing sintering temperature, the $Q \times f$ increased to a maximum value at 1200 °C and thereafter it decreased. The variation of $Q \times f$ was also consistent with that of density suggesting it was mainly dominated by the density of the specimens. In fact, apparent density plays an important role in controlling the dielectric loss, which has been shown for other microwave dielectric materials. The decrease in $Q \times f$ value was due to the inhomogeneous grain growth result-

ing in a lower density, as observed in Figs. 3 and 6. It has been reported [23,24] that the microwave dielectric loss is mainly caused not only by the lattice vibration modes, but also by the pores, the second phases, the impurities or the lattice defect. Higher B_2O_3 content would degrade the $Q \times f$ value of 92MCT–8CST ceramics, which is most likely due to the low $Q \times f$ of liquid phase. Recently, Alford and colleagues [25] also conclude that the grain boundaries have a very limited influence on the microwave dielectric loss while impurities and porosity are particularly deleterious to microwave loss in their recent studies, which also confirms our results. Furthermore, the temperature coefficient of resonant frequency is well known to be governed by the composition, the additives, and the second phase of the materials. The τ_f moves toward positive as the B_2O_3 content increases implying the formation of liquid phase shifts the τ_f to positive. In addition, significant

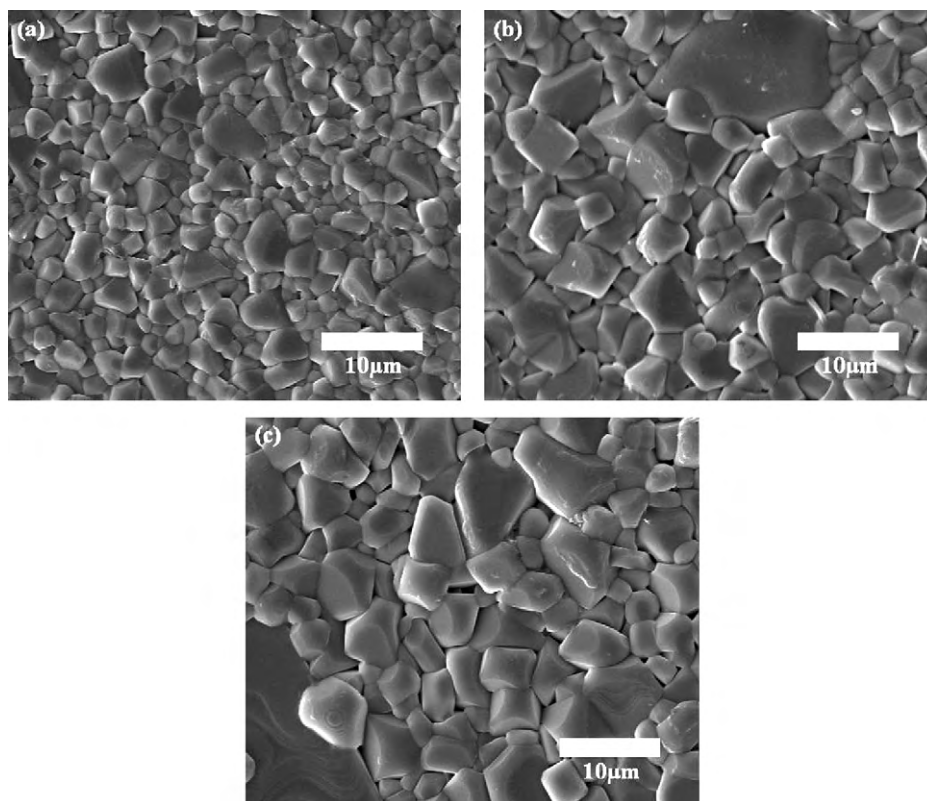


Fig. 4. SEM micrographs of $0.92(\text{Mg}_{0.95}\text{Co}_{0.05})_2\text{TiO}_4-0.08(\text{Ca}_{0.8}\text{Sr}_{0.2})\text{TiO}_3$ ceramics with (a) 0.5 wt%, (b) 1.0 wt% and (c) 2.0 wt% B_2O_3 additions sintered at 1200°C for 4 h.

variance in the τ_f was not observed for specimens at different sintering temperatures. With 0.5 wt% B_2O_3 addition, a τ_f value of -4.7 ppm/ $^\circ\text{C}$ was obtained for 92MCT–8CST ceramics at 1200°C for 4 h.

The influence of sintering time on the microwave dielectric properties of 0.5 wt% B_2O_3 -doped 92MCT–8CST is also investigated and illustrated in Table 2. The optimal microwave dielectric properties are achieved for specimen sintered at 1200°C for 4 h. It possesses a dielectric constant (ϵ_r) of ~ 18.07 , a $Q \times f$ value

Table 1

The EDX data of the spots A–F shown in Fig. 5.

Spots	Atom (%)						
	Mg K	Co K	Ca K	Sr L	Ti K	B K	O K
A	27.80	1.57	0	0	15.95	1.03	53.65
B	29.42	1.49	0	0	17.11	0.61	51.37
C	28.05	1.63	0	0	16.93	0.72	52.67
D	0	0	16.90	5.12	20.47	0.56	56.95
E	0	0	18.13	6.01	21.70	1.15	53.01
F	0	0	15.97	4.56	20.95	0.75	57.77

Table 2

Microwave dielectric properties of 0.5 wt% B_2O_3 -doped $0.92(\text{Mg}_{0.95}\text{Co}_{0.05})_2\text{TiO}_4-0.08(\text{Ca}_{0.8}\text{Sr}_{0.2})\text{TiO}_3$ ceramics sintered at 1200°C with different sintering time.

Time (h)	Apparent density (g/cm^3)	ϵ_r	$Q \times f$ (GHz)	τ_f (ppm/ $^\circ\text{C}$)
2.0	3.38	17.92	80,200	-3.9
4.0	3.45	18.07	95,000	-4.7
6.0	3.42	18.00	72,600	-6.2

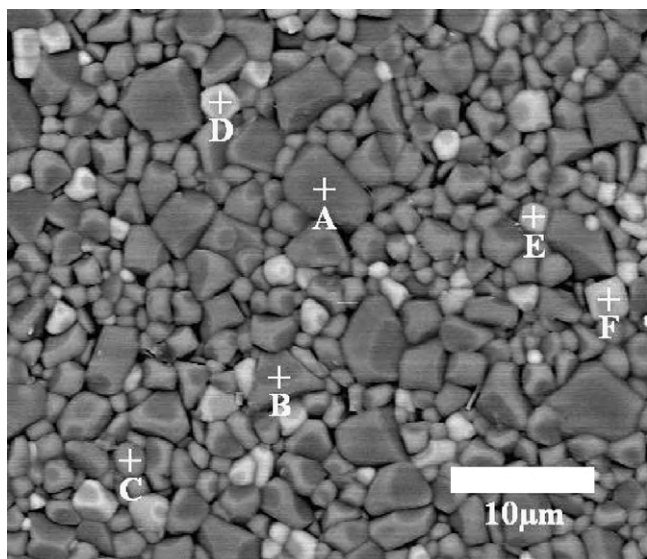


Fig. 5. The marks of backscattering electron image (BEI) for the 0.5 wt% B_2O_3 -doped $0.92(\text{Mg}_{0.95}\text{Co}_{0.05})_2\text{TiO}_4-0.08(\text{Ca}_{0.8}\text{Sr}_{0.2})\text{TiO}_3$ ceramics sintered at 1200°C for 4 h.

of $\sim 95,000$ GHz (at 9.5 GHz) and a temperature coefficient of resonant frequency (τ_f) of ~ -4.7 ppm/ $^\circ\text{C}$. In comparison with other similar ceramic system [26–29] (Table 3), the B_2O_3 -doped 92MCT–8CST shows the highest $Q \times f$ at a comparably low sintering temperature.

To verify the performance of the proposed material, a band-pass filter is designed for a center frequency of 2.4 GHz and fabricated on FR4, Al_2O_3 and 92MCT–8CST (0.5 wt% B_2O_3). Fig. 8 shows the physical layout of the designed filter with a center frequency of 2.4 GHz. The simulation results are listed in Table 4. Compared to FR4 and Al_2O_3 , the filter using the 92MCT–8CST (0.5 wt% B_2O_3)

Table 3
Comparison of the proposed dielectrics with other similar ceramic systems.

Compound	ϵ_r	$Q \times f$ (GHz)	τ_f (ppm/°C)	Sintering temperature (°C)	Ref.
0.92(Mg _{0.95} Co _{0.05})TiO ₃ –0.08CaTiO ₃	21.6	92,000	–1.8	1275	[26]
0.93(Mg _{0.95} Zn _{0.05})TiO ₃ –0.07CaTiO ₃	22.6	93,000	–2.6	1300	[27]
0.94(Mg _{0.95} Ni _{0.05})TiO ₃ –0.06CaTiO ₃	20.9	79,200	1.2	1300	[28]
0.93(Mg _{0.95} Mn _{0.05})TiO ₃ –0.07CaTiO ₃	22.6	90,700	0.8	1270	[29]
0.92(Mg _{0.95} Co _{0.05}) ₂ TiO ₄ –0.08(Ca _{0.8} Sr _{0.2})TiO ₃ + B ₂ O ₃	18.07	95,000	–4.7	1200	This work

Table 4
Simulation results of the band-pass filters using different dielectrics.

Substrate	ϵ_r	$\tan \delta$	f_0 (GHz)	S_{11} (dB)	S_{21} (dB)	Size (mm ²) $a \times b$
FR4	4.4	0.02	2.4	–23.55	–3.20	13.5 × 26.4
Al ₂ O ₃	9.8	0.0005	2.4	–22.60	–0.91	9.29 × 19.35
92MCT–8CST+0.5 wt% B ₂ O ₃	18.07	0.0001	2.4	–26.36	–0.85	6.84 × 14.07

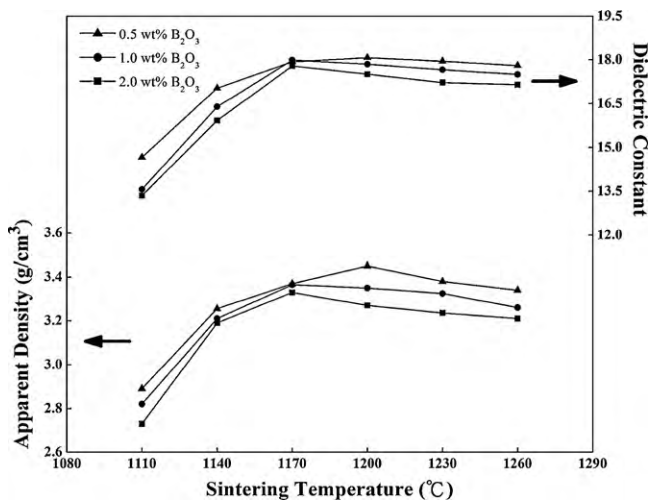


Fig. 6. Apparent densities and dielectric constants of doped 0.92(Mg_{0.95}Co_{0.05})₂TiO₄–0.08(Ca_{0.8}Sr_{0.2})TiO₃ ceramics as a function of its sintering temperature.

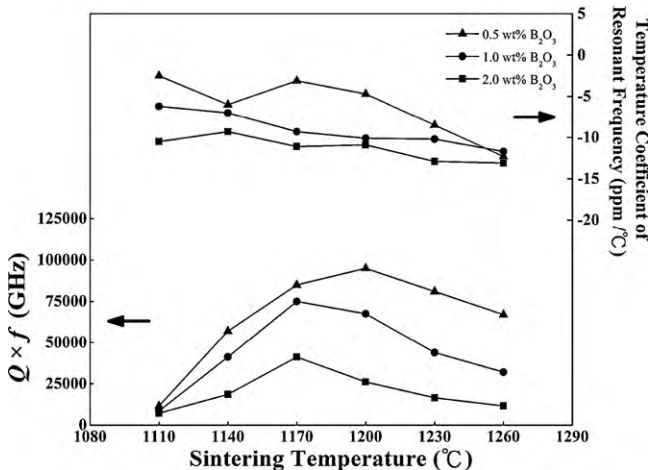


Fig. 7. $Q \times f$ and τ_f values of doped 0.92(Mg_{0.95}Co_{0.05})₂TiO₄–0.08(Ca_{0.8}Sr_{0.2})TiO₃ ceramics as a function of its sintering temperature.

ceramic shows a tremendous reduction in the insertion loss and demonstrates a large reduction in its size. This design approach enables one to use an EM simulator (IE3D) to complete the filter design in order to determine the physical dimensions of the filters.

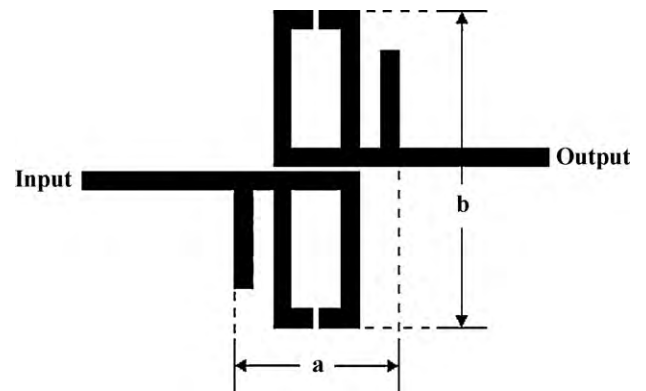


Fig. 8. Physical layout of the band-pass filter.

4. Conclusion

The microstructures and the microwave dielectric properties of B₂O₃-doped 92MCT–8CST ceramics were investigated. The dielectric properties of 92MCT–8CST dielectric materials were determined by the sintering conditions and the content of sintering aid. A substantial sintering temperature reduction (100 °C) can be achieved by adding B₂O₃ to the 92MCT–8CST ceramics. With 0.5 wt% B₂O₃ addition, a dielectric constant (ϵ_r) of 18.07, a $Q \times f$ value of 95,000 (at 9.5 GHz) and a τ_f of –4.7 ppm/°C can be achieved for 92MCT–8CST sintered at 1200 °C for 4 h. Compared to that of FR4 and Al₂O₃, the filter using 92MCT–8CST (+0.5 wt% B₂O₃) ceramic substrate shows a tremendous reduction in the insertion loss and demonstrates a large reduction in its size suggesting the proposed dielectric can find applications requiring high operation frequencies.

Acknowledgement

This work was supported by the National Science Council of Taiwan under grant NSC 97-2221-E-006-013-MY3.

References

- [1] G.G. Yao, P. Liu, *Physica B* 405 (2010) 547–551.
- [2] C.L. Huang, T.J. Yang, C.C. Huang, *J. Am. Ceram. Soc.* 92 (2009) 119–124.
- [3] C.L. Huang, J.J. Wang, C.Y. Huang, *J. Am. Ceram. Soc.* 90 (2007) 1487–1493.
- [4] B.L. Liang, X.H. Zheng, D.P. Tang, *J. Alloys Compd.* 488 (2009) 409–413.
- [5] M.S. Fu, X.Q. Liu, X.M. Chen, Y.W. Zeng, *J. Am. Ceram. Soc.* 91 (2008) 1163–1168.
- [6] C.L. Huang, J.Y. Chen, Y.H. Wang, *J. Alloys Compd.* 478 (2009) 842–846.
- [7] C.L. Huang, J.Y. Chen, *J. Am. Ceram. Soc.* 93 (2010) 470–473.

- [8] Y.C. Chen, S.M. Tsao, C.S. Lin, S.C. Wang, Y.H. Chien, J. Alloys Compd. 471 (2009) 347–351.
- [9] J.H. Sohn, Y. Inaguma, S.O. Yoon, M. Itoh, T. Nakamura, S.J. Yoon, H.J. Kim, Jpn. J. Appl. Phys. 33 (1994) 5466–5470.
- [10] A. Belous, O. Ovchar, D. Durylin, M. Valant, M.M. Krzmann, D. Suvorov, J. Eur. Ceram. Soc. 27 (2007) 2963–2966.
- [11] A. Belous, O. Ovchar, D. Durylin, M.M. Krzmann, M. Valant, D. Suvorov, J. Am. Ceram. Soc. 89 (2006) 3441–3445.
- [12] C.L. Huang, J.Y. Chen, J. Am. Ceram. Soc. 92 (2009) 675–678.
- [13] C.L. Huang, J.Y. Chen, J. Am. Ceram. Soc. 92 (2009) 379–383.
- [14] P.L. Wise, I.M. Reaney, W.E. Lee, T.J. Price, D.M. Iddles, D.S. Cannell, J. Eur. Ceram. Soc. 21 (2001) 1723–1726.
- [15] C.L. Huang, S.S. Liu, J. Alloys Compd. 471 (2009) L9–L12.
- [16] S.Y. Cho, H.J. Youn, H.J. Lee, K.S. Hong, J. Am. Ceram. Soc. 84 (2001) 753–758.
- [17] C.L. Huang, J.Y. Chen, B.J. Li, J. Alloys Compd. 484 (2009) 494–497.
- [18] J.Y. Chen, B.J. Li, C.L. Huang, A novel low-loss microwave dielectric using $(\text{Ca}_{0.8}\text{Sr}_{0.2})\text{TiO}_3$ -modified $(\text{Mg}_{0.95}\text{Co}_{0.05})_2\text{TiO}_4$ ceramics, J. Alloys Compd., doi:10.1016/j.jallcom.2010.02.041.
- [19] S.P. Wu, J. Ni, J.H. Luo, X.H. Ding, Mater. Chem. Phys. 117 (2009) 307–312.
- [20] C.L. Huang, K.H. Chiang, Mater. Res. Bull. 39 (2004) 1701–1708.
- [21] B.W. Hakki, P.D. Coleman, IEEE Trans. Microw. Theory Tech. 8 (1960) 402–410.
- [22] W.E. Courtney, IEEE Trans. Microw. Theory Tech. 18 (1970) 476–485.
- [23] B.D. Silverman, Phys. Rev. 125 (1962) 1921–1930.
- [24] H. Tamura, J. Eur. Ceram. Soc. 26 (2006) 1775–1780.
- [25] J.D. Breeze, J.M. Perkins, D.W. McComb, N.McN. Alford, J. Am. Ceram. Soc. 92 (2009) 671–674.
- [26] C.L. Huang, C.L. Pan, J.F. Hsu, Mater. Res. Bull. 37 (2002) 2483–2490.
- [27] C.L. Huang, S.S. Liu, Mater. Lett. 62 (2008) 3773–3775.
- [28] C.H. Shen, C.L. Huang, J. Alloys Compd. 472 (2009) 451–455.
- [29] C.L. Huang, J.Y. Chen, G.S. Huang, J. Alloys Compd. 499 (2010) 48–52.